COMMUNICATION

ChemComm
www.rsc.org/chemcomm

High efficiency photocurrent generation by two-dimensional mixed J-aggregates of cyanine dyes

Mitsuo Kawasaki* and Satoshi Aoyama

Department of Molecular Engineering, Graduate School of Engineering, Kyoto University, Katsura, Kyoto 615-8510, Japan. E-mail: Kawasaki@ap6.kuic.kyoto-u.ac.jp; Fax: (+81)75-383-2574; Tel: (+81)75-383-2574

Received (in Cambridge, UK) 7th January 2004, Accepted 2nd March 2004
First published as an Advance Article on the web 19th March 2004

Two-dimensional mixed J-aggregates of structurally and spectrally analogous anionic cyanine dyes, coadsorbed on a self-assembled monolayer of aminoalkanethiolate on Au(111), generated a high-efficiency (20–30% quantum efficiency) cathodic photocurrent and a significant photovoltaic effect in reversible Fe^{2+}/Fe^{3+} redox solution.

The photoinduced electron transfer at self-assembled monolayers (SAMs) of photo- and redox-active organic molecules has been of considerable interest for such potential applications as photonic molecular devices and artificial photosynthetic systems.[1] The intensive effort to control the multistep electron transfer in complex molecular assemblies of donor–acceptor-linked compounds unidirectionally organized on gold electrodes led to the photocurrent quantum yield, 11–25%[2,3] or more,[4] though the incident photon-to-photocurrent efficiency (IPCE) is still limited to ~2% at most. Here, we newly illuminate an equally or more efficient photoelectric conversion by a much simpler system comprising two-dimensional (2D) mixed J-aggregates of structurally and spectrally analogous cyanine dyes (**1** and **2**) organized above Au(111) with an intermediate SAM spacer of aminoalkanethiols (**3a,b**).

An atomically flat, ~200 nm thick, Au(111) electrode was prepared by the DC Ar^+ ion sputtering method[5] on freshly cleaved natural mica. It was immersed in an 0.1 mM ethanolic solution of **3** (obtained as hydrochloride salts from Dojindo Laboratories) at room temperature for 5–10 min to obtain a densely amino-functionalized Au(111) surface. Subsequent coadsorption of **1** and **2** (obtained from Hayashibara Biochemical Laboratories, Inc.) from 0.1 mM mixed dye solution in 1 : 1 water/ethanol solvent (~5 min at 50 °C) led to the formation of well-mixed 2D J-aggregates electrostatically bound to the SAM of **3** by ammonium sulfonate linkage.[6] The resultant total dye coverage (~1.3×10^{14} molecules cm^{-2}) and the actual **1** : **2** molar ratio in the mixed J-aggregate were estimated by direct spectrophotometric quantification of the adsorbed dyes re-extracted into ethanol solvent. The estimated dye coverage agrees with a face-to-face dense packing (with 3–4 Å spacing) of edge-on dye molecules characteristic of 2D J-aggregate. The absorption spectra of the **1–2** mixed J-aggregates on the Au electrode (nontransparent) were taken in the reflection mode at normal incidence. The spectra (in reflection absorbance†) invariably exhibited a single J-band (Fig. 1b) largely red-shifted from the monomer bands (550–570 nm) at an intermediate position between those associated with single-component J-aggregates of **1** (~654 nm) and **2** (~664 nm). This strongly suggests that the excited state of the **1–2** mixed J-aggregate makes a unique molecular exciton delocalized over both **1** and **2**.

The aqueous electrolyte solution for the photoelectrochemical measurement consisted of $FeSO_4$, $Fe_2(SO_4)_3$, and $CH_2(COONa)_2$ (effective chelating agent for Fe^{3+}) with the total concentration of Fe^{2+} and Fe^{3+} ions typically 0.25 M, and that of malonates 0.7–1.7 M. The corresponding redox potential changed in a wide range (~0 to ~0.45 V *vs.* Ag|AgCl) according to the Fe^{2+}/Fe^{3+} ratio (typically 1/5) and the relative content of malonates. Besides, the presence of excess malonates of the order of 1 M effectively prevented dissolution of the 2D J-aggregate, which was rather loosely (electrostatically) bound to the SAM of **3**. The photocurrent measurements were first carried out in the potentiostat mode by using a three-electrode cell with an Ag|AgCl reference and a Pt counter electrode, under 1.2 mW monochromatic irradiation focused onto an area of ~0.07 cm^2 (corresponding to ~20 mW cm^{-2} power density).

Fig. 1a shows typical examples of markedly large photocurrent (cathodic) signals well exceeding 10 μA, obtained at the J-band peak for the mixed 2D J-aggregate of 19(**1**) : 6(**2**) molar ratio. The redox solution used here had a relatively positive redox potential of 0.37 V *vs.* Ag|AgCl. The zero dark current means that the applied electrode potential was set equal to this equilibrium potential. In other potential conditions, there occurred also significant dark current not completely blocked by the SAM of **3**. The net photocurrent relative to the dark remained approximately constant, however, except in the potential region more positive than the equilibrium potential. Fig. 1a also suggests an important role of the alkyl chain length of the intermediate SAM spacer, the longer one (**3b**) leading to a significantly higher photocurrent close to 20 μA. However, the corresponding J-aggregate underwent considerably faster degradation (resulting in a gradual decrease in photocurrent) upon continued irradiation, which is noticeable even in the given time scale of ~10 s in Fig. 1a. The stability of the J-aggregate against this photodegredation could be significantly improved by increasing the malonate content in the redox solution, but the concomitant negative shift in its redox potential inevitably reduced

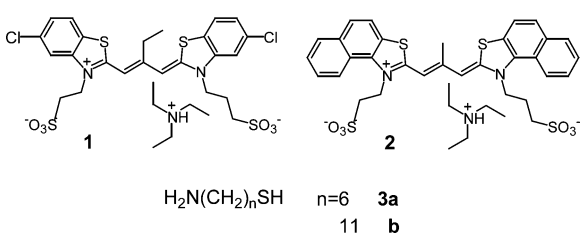

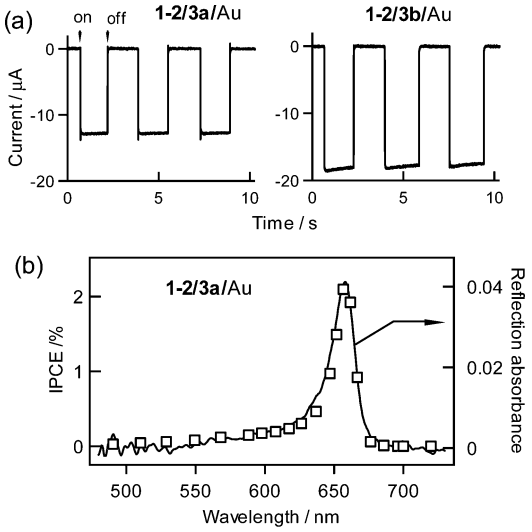

Fig. 1 (a) Examples of cathodic photocurrent signals for pulsed light (1.2 mW) irradiation at the J-band peak (657 nm). (b) Comparison between photocurrent action spectrum in IPCE (open squares) and absorption spectrum (solid line) of a mixed 2D J-aggregate.

DOI: 10.1039/b400071d

the photocurrent, *e.g.*, by factor of ~2 in solution with a redox potential of 0.1 V *vs.* Ag|AgCl.

We also confirmed a good agreement between the photocurrent action spectrum (in IPCE) and the J-band, as shown in Fig. 1b. This proves that the reflection absorbance properly scales to the net light absorption by the 2D J-aggregate on Au(111), which we estimate to be ~10%‡ at the J-band peak in Fig. 1b. Then the photocurrent signals shown in Fig. 1a correspond to quantum efficiency (QE) in the 20–30% range. Table 1 summarizes the thus estimated average QE (together with peak IPCE) for the **1–2** mixed aggregate in comparison with those of single-component aggregates. The reproducibility for a number of similarly prepared samples was better than ±10%. It can be seen that the 19 : 6 mixing of **1** and **2** caused 4–5 times photocurrent enhancement as compared to the single-component aggregates. It should be also emphasized that the spacing between the Au surface and the present 2D J-aggregate (could be less than 20 Å even with the longer-chain SAM spacer of **3b**) is so small that the dye-to-metal energy transfer still remains as the major deactivation channel of the excited J-aggregate. A maximum of ~30% photocurrent QE achievable in this situation is particularly remarkable.

This high QE for the mixed J-aggregate may be rationalized by the oxidation potential data for the monomers of **1** and **2** (0.94 and 0.76 V *vs.* Ag|AgCl)[7,8] and their 2D J-aggregates (0.82 and 0.57 V *vs.* Ag|AgCl),[9] establishing that **2** is more easily oxidized than **1**. Furthermore, the excited state of the **1–2** mixed J-aggregate likely forms a shared molecular exciton delocalised over both **1** and **2**, as mentioned already. We therefore suggest that this mixed excitonic state can undergo a very fast (so as to compete well with the dye-to-metal energy transfer) [intra-aggregate] charge separation into an electron and a hole discretely localized at the sites of **1** and **2**, respectively. The subsequent rapid electron transfer from $\mathbf{1}^-$ to Fe^{3+} ion in solution, followed by a relatively slow electron tunnelling from Au to $\mathbf{2}^+$ through the SAM spacer, then gives rise to the high-efficiency cathodic photocurrent in a vectorial manner. The enhanced intra-aggregate charge separation would be supported further if we could verify a stronger fluorescence quenching in the mixed aggregates; but unfortunately, this was difficult with our steady-state fluorescence measurement because the dye-to-metal energy transfer alone already caused too weak a fluorescence signal below our detection limit.

Importantly, the present system with a reversible Fe^{2+}/Fe^{3+} redox solution meets the condition for it to serve also as a two-electrode photovoltaic cell. The high efficiency cathodic photocurrent suggests that the backward electron transfer from Fe^{2+} ions to dye positive hole ($\mathbf{2}^+$) is effectively suppressed somehow in the present system. Thus Fe^{3+} ions are preferentially reduced at the photocathode, whereas the oxidation of Fe^{2+} ions predominates at the counter electrode, to keep an overall constant solution composition. Fig. 2 shows examples of such photovoltaic *I–V* curves obtained for the **1–2** mixed J-aggregate and for the single-component J-aggregate of **2**. Here, the shorter SAM spacer (**3a**) and a more negative (0.22 V *vs.* Ag|AgCl) redox solution with increased malonate content (1.65 M) were chosen to ensure good stability of the cell during the *I–V* measurement at the expense of photocurrent.

Table 1 Photocurrent QE (peak IPCE) (%)[a] for single-component and mixed J-aggregate films

1/3a/Au	**2/3a/Au**	**1–2/3a/Au**
3.8 (0.6)	5.4 (0.5)	20 (2.0)[b]
1/3b/Au	**2/3b/Au**	**1–2/3b/Au**
5.0 (0.8)	7.6 (0.6)	28 (2.7)[b]

[a] In 0.25 M Fe^{3+}/Fe^{2+} redox solution with 1.1 M malonates (0.37 V *vs.* Ag|AgCl). [b] At optimum **1** : **2** mixing ratio of 19 : 6.

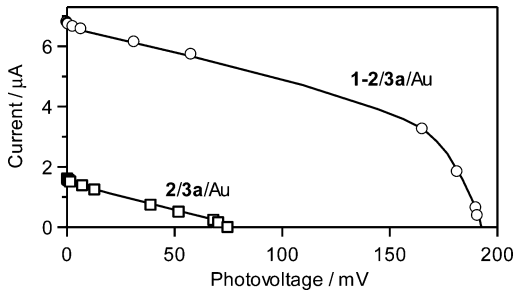

Fig. 2 Examples of photovoltaic *I–V* curves obtained in a simple two-electrode cell with a Pt counter electrode, for input energy of 1.2 mW at the J-band peak.

As expected, the short-circuit current (I_{sc}) for each sample was similar to that measured in the potentiostat mode. The open-circuit voltage (V_{oc}) strongly depended on I_{sc}, causing much smaller V_{oc} with a single-component J-aggregate. This can be understood from the following mechanism of the photovoltaic effect, which is fundamentally different from that in the well-established dye-sensitized TiO_2 solar cells.[10] The photovoltage here is developed across the SAM spacer as the cathodic photocurrent lowers the Au Fermi level relative to the solution. This in turn increases the reverse dark current due to Fe^{2+} ions through the more-or-less imperfect SAM spacer. In the present conditions,§ V_{oc} is determined kinetically by the balance of these counteracting currents, so it naturally depends on I_{sc}, and on the magnitude of dark current influenced by the quality of SAM spacer.

The maximum output power derived under the *I–V* curve shown in Fig. 2 for the **1–2** mixed J-aggregate (I_{sc} ~ 7 μA and V_{oc} ~ 190 mV) is ~0.6 μW (for 1.2 mW input energy), so the photoelectric power conversion efficiency remains as small as 0.05%. This is due primarily to the limited IPCE presently available, which in turn limits also V_{oc}. Nevertheless, the modest but substantial photovoltaic effect clearly evidenced here with such a simple chemically-modified gold electrode further adds to the specialty of the **1–2** type mixed J-aggregate as a unique light-absorbing and redox-active molecular assembly.

Notes and references

† Defined by log (R_0/R), with R_0 and R for the reflectance values of the Au electrode before and after dye adsorption.

‡ Our Au(111) film has a high reflectance (R_0) more than 90% at wavelengths longer than 600 nm. Then, the overall increase in light absorption by dye-coated Au, given by $R_0 - R$, may be associated almost entirely with the J-aggregate, or at least gives the upper limit of light absorption by the J-aggregate. The estimated QE in Table 1 is more like the lower limit in the latter sense.

§ In the high I_{sc} limit not yet reached here, V_{oc} should be limited by the difference between the solution redox potential and the dye (**2**) oxidation potential, around ~400 mV with the solution used in Fig. 2.

1 H. Imahori, Y. Mori and Y. Matano, *J. Photochem. Photobiol.*, 2003, **4**, 51.
2 K. Uosaki, T. Kondo, X-Q. Zhang and M. Yanagida, *J. Am. Chem. Soc.*, 1997, **119**, 8367.
3 H. Imahori, H. Yamada, S. Ozawa, K. Ushida and Y. Sakata, *Chem. Commun.*, 1999, 1165.
4 H. Imahori, H. Norieda, H. Yamada, Y. Nishimura, I. Yamazaki, Y. Sakata and S. Fukuzumi, *J. Am. Chem. Soc.*, 2001, **123**, 100.
5 M. Kawasaki and H. Uchiki, *Surf. Sci.*, 1997, **388**, L1121.
6 M. Kawasaki, T. Sato and T. Yoshimoto, *Langmuir*, 2000, **16**, 5409.
7 J. Lenhard, *J. Imaging Sci.*, 1986, **30**, 27.
8 T. Tani, K. Ohzeki and K. Seki, *J. Electrochem. Soc.*, 1991, **138**, 1411.
9 M. Kawasaki, D. Yoshidome, T. Sato and M. Iwasaki, *J. Electroanal. Chem.*, 2003, **543**, 1.
10 A. Hagfeldt and M. Graetzel, *Chem. Rev.*, 1995, **95**, 49.